

# Effectiveness Assessment of Recent Large Vision-Language Models

Yao Jiang<sup>†</sup>, Xinyu Yan<sup>†</sup>, Ge-Peng Ji, Keren Fu<sup>\*</sup>, Meijun Sun, Huan Xiong<sup>\*</sup>,  
Deng-Ping Fan<sup>‡</sup>, Fahad Shahbaz Khan

**Abstract**—The advent of large vision-language models (LVLMs) represents a noteworthy advancement towards the pursuit of artificial general intelligence. However, the extent of their efficacy across both specialized and general tasks warrants further investigation. This article endeavors to evaluate the competency of popular LVLMs in specialized and general tasks, respectively, aiming to offer a comprehensive comprehension of these innovative methodologies. To gauge their efficacy in specialized tasks, we tailor a comprehensive testbed comprising three distinct scenarios: natural, healthcare, and industrial, encompassing six challenging tasks. These tasks include salient, camouflaged, and transparent object detection, as well as polyp and skin lesion detection, alongside industrial anomaly detection. We examine the performance of three recent open-source LVLMs – MiniGPT-v2, LLaVA-1.5, and Shikra – in the realm of visual recognition and localization. Moreover, we conduct empirical investigations utilizing the aforementioned models alongside GPT-4V, assessing their multi-modal understanding capacities in general tasks such as object counting, absurd question answering, affordance reasoning, attribute recognition, and spatial relation reasoning. Our investigations reveal that these models demonstrate limited proficiency not only in specialized tasks but also in general tasks. We delve deeper into this inadequacy and suggest several potential factors, including limited cognition in specialized tasks, object hallucination, text-to-image interference, and decreased robustness in complex problems. We hope this study would provide valuable insights for the future development of LVLMs, augmenting their power in coping with both general and specialized applications.

**Index Terms**—Large vision-language models, recognition, localization, multi-modal understanding



## 1 INTRODUCTION

The emergence of large language models (LLMs) [1], [2] has sparked a revolution in the realm of natural language processing, owing to their promising generalization and reasoning capabilities. Motivated by this progress, researchers have pioneered the development of powerful large vision-language models (LVLMs) [3], [4], [5], leveraging the impressive capabilities of LLMs to enhance the comprehension of visual semantics. This advancement notably elevates model performance in complex vision-language tasks [4], [6], [7], signifying a significant step towards the realization of artificial general intelligence (AGI). In general, the capabilities of LVLMs can be broadly categorized into two groups: general capabilities [4], [5], which encompass tasks of a more universal nature, and specialized capabilities [8], [9], which pertain to tasks with domain-specific expertise.

Both specialized and general capabilities are integral components on the path towards achieving AGI. Specialized capabilities are imperative for making strides in specific domains, while general capabilities serve as the bedrock of knowledge and understanding, facilitating progress across diverse domains. Recently, numerous studies have extensively assessed and investigated the general and specialized capabilities of LVLMs. However, a majority of these studies primarily focus on the application of models within a single professional domain [8], [9], [10], [11] or assess their general abilities [6], [7]. In this article, we embark on comprehensive assessment of various recent open-source LVLMs, spanning a diverse array of challenging specialized tasks and generic tasks.

Our evaluation platform is illustrated in Fig. 1. To assess the proficiency of LVLMs in specialized tasks, we select three recent open-source LVLMs (MiniGPT-v2 [4], LLaVA-1.5 [12], and Shikra [13]) and conduct comprehensive assessment using a tailored testbed. This testbed comprises six challenging specialized tasks distributed across three diverse scenarios (natural, healthcare, and industrial). In natural scenes, we focus on salient object detection (SOD) [15], transparent object detection (TOD) [16], and camouflaged object detection (COD) [17], [18], considering the target objects ranging from frequently occurring ones to those more infrequent and challenging ones. In the field of healthcare, the aimed objects span from skin lesions [19] that exhibit prominent visual characteristics and therefore are easier to detect, to increasingly intricate and specialized polyps [20]. Besides, we incorporate anomaly detection (AD) [21], a task vital in industrial scenarios, to assess the performance of

- Yao Jiang is with Mohamed Bin Zayed University of Artificial Intelligence, Abu Dhabi, UAE, and Sichuan University, Chengdu, China.
- Xinyu Yan is with Mohamed Bin Zayed University of Artificial Intelligence, Abu Dhabi, UAE, and Tianjin University, Tianjin, China.
- Ge-Peng Ji is with Australian National University, Canberra, Australia.
- Keren Fu is with Sichuan University, Chengdu, China.
- Meijun Sun is with Tianjin University, Tianjin, China.
- Huan Xiong is with Mohamed Bin Zayed University of Artificial Intelligence, Abu Dhabi, UAE, and Harbin Institute of Technology, Harbin, China.
- Deng-Ping Fan is with Nankai University, Tianjin, China.
- Fahad Shahbaz Khan is with Mohamed Bin Zayed University of Artificial Intelligence, Abu Dhabi, UAE.
- <sup>†</sup> Two authors contribute equally. <sup>‡</sup> Deng-Ping Fan is the project lead.
- <sup>\*</sup> Corresponding authors: Keren Fu (fksuper@scu.edu.cn) and Huan Xiong (huan.xiong.math@gmail.com). Work was done while Yao Jiang and Xinyu Yan were MBZUAI visiting scholars.

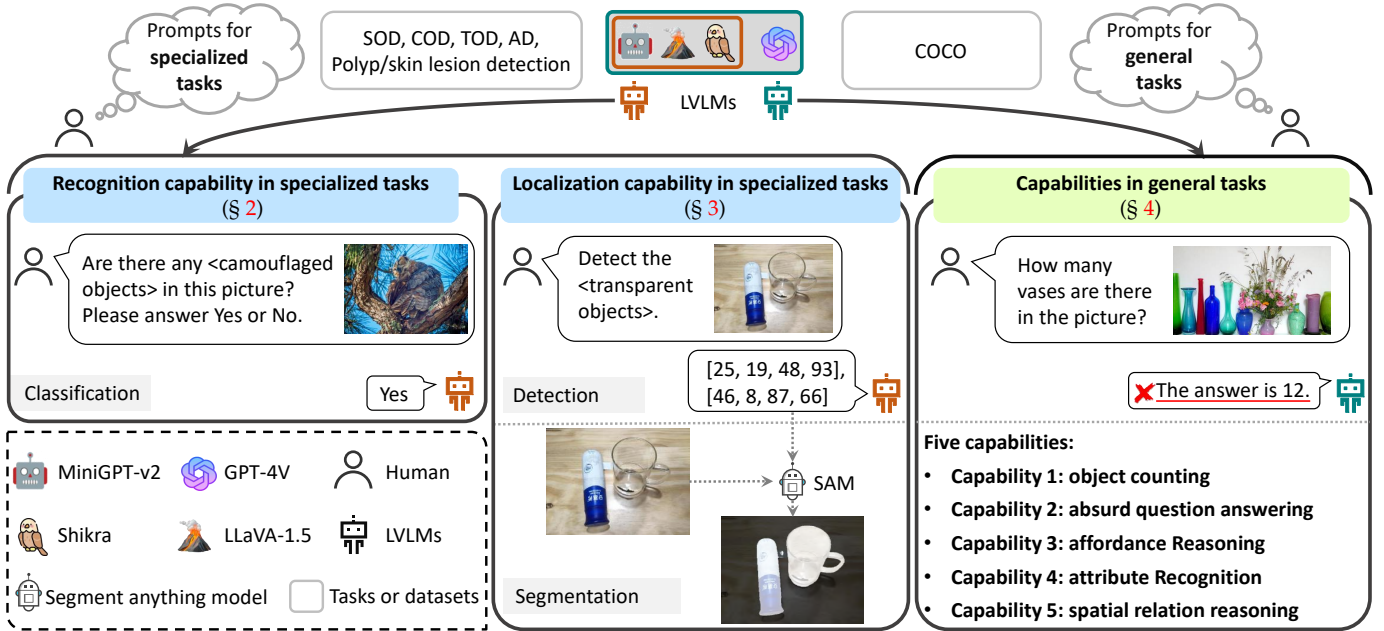


Fig. 1. Overall diagram of our evaluation platform. We assess the proficiency of recent LVLMs in both specialized and general tasks using tailored prompts, with and without specifying specific attributes of objects. Three recent open-source LVLMs (MiniGPT-v2 [4], LLaVA-1.5 [12], and Shikra [13]) undergo evaluation on a tailored testbed comprising six specialized tasks: salient object detection (SOD), transparent object detection (TOD), camouflaged object detection (COD), polyp and skin lesion detection, as well as industrial anomaly detection (AD). This evaluation aims to assess their recognition (§ 2) and localization (§ 3) capabilities. Empirical investigations are also conducted on the COCO [14] dataset to evaluate the capabilities of LVLMs in general tasks (§ 4), including object counting, absurd question answering, affordance reasoning, attribute recognition, and spatial relation reasoning. Examples of evaluations are presented in each figure group, where “<...>” indicates a placeholder that can be replaced with other words/phrases in different tasks.

LVLMs. These six commonly encountered computer vision tasks, which come with specialized datasets, cover a broad spectrum of specialized domains and enable comprehensive validation of the specialized capabilities inherent in LVLMs. As illustrated in Fig. 1, given inherent challenges posed by these tasks in terms of recognizing and localizing objects with specific attributes, we employ tailored prompts featuring specific attributes of objects to assess the recognition (§ 2) and localization (§ 3) capabilities of the models. Furthermore, we conduct empirical investigations on a universal dataset (COCO [14]) that is devoid of domain-specific expertise. We abstain from specifying particular attributes in prompts, aiming to explore multi-modal understanding capabilities (§ 4) of the above-mentioned models and widely-recognized GPT-4V in general tasks (*i.e.*, object counting, absurd question answering, affordance reasoning, attribute recognition, and spatial relation reasoning).

Our investigations reveal that while these models exhibit strong potential for specialized tasks when directly applied without fine-tuning and training, they still demonstrate suboptimal performance and limited cognitive abilities. This reveals their inadequate generalization capacity in this particular context. Performance issues are further magnified by typical weaknesses of LVLMs such as object hallucination, text-to-image interference, and decreased robustness in complex problems. In addition to shortcomings exposed in specialized tasks, these models also show significant room to improve in general tasks, particularly in object counting, spatial reasoning, and absurd question answering. In summary, in this study, we assess the proficiency of three open-source LVLMs on six challenging specialized tasks

and four LVLMs on several general tasks. We anticipate that our study will provide valuable insights for the future development of LVLMs, encompassing both general and specialized capabilities.

## 2 RECOGNITION VIA LVLMS IN SPECIALIZED TASKS

When LVLMs are applied in these specialized tasks, the recognition of objects with specific attributes plays a crucial role. It reflects models’ understanding of such tasks and directly influences their overall effectiveness and practicality. In this chapter, we initially conduct a quantitative evaluation of their recognition capabilities in specialized tasks using the tailored testbed. Subsequently, we carry out additional tests to delve into failure cases and gain further insights.

### 2.1 Quantitative Investigation

#### 2.1.1 Experimental Setup

Recognition in specialized tasks involves various aspects, including but not limited to determining the existence of targets and classifying them. Our initial evaluation of recognition capabilities involves utilizing models to ascertain target existence. This evaluation is structured as an existence determination task (binary classification), requiring models to answer either “Yes” or “No” response to queries like “Are there any <camouflaged objects> in the picture? Please answer Yes or No.” as demonstrated in Fig. 1. The placeholder “<...>” within queries denote flexible elements that can

be substituted with alternative words/phrases depending on the specific tasks, such as “polyps” in polyp detection. We comprehensively explore their recognition capabilities in two distinct scenarios: the full set, encompassing both positive and negative samples, and the positive set, only comprising positive samples.

Beyond recognizing the presence of targets, we delve deeper into the intricate realm of LVLMs’ recognition prowess by tasking them with categorizing targets. An elementary methodology for assessing this involves prompting models to designate the most suitable category for the target from a predefined set of potential categories (*w/ vocabulary*). Within this experiment, the inquiry resembles, “Which of the following is the most likely category for the camouflaged object in the picture? ‘seahorse, mantis, spider ...’”. The predefined vocabulary set encompasses all categories that are present in the dataset. Nonetheless, occasional missteps may occur wherein LVLMs may produce categories not included among the candidates, resulting in similar yet inconsistent categorizations for an object. Hence, an additional evaluation is conducted, featuring an open-vocabulary inquiry without offering a predefined set (*w/o vocabulary*). In this examination, a straightforward question like “What is the camouflaged object in the picture?” is posed to elicit the target category.

### 2.1.2 Metrics

In the existence determination experiment, accuracy ( $\mathcal{A}$ ) is employed as the metric to gauge recognition capabilities in specialized tasks. Moreover, for reference, we present the probability of positive responses (responses indicating “yes”) on the full set, denoted as  $\mathcal{Y}$ .  $\mathcal{A}$  and  $\mathcal{Y}$  can be expressed as follows:

$$\mathcal{A} = \frac{TP + TN}{TP + FP + TN + FN}, \quad (1)$$

$$\mathcal{Y} = \frac{TP + FP}{TP + FP + TN + FN}, \quad (2)$$

where  $TP$ ,  $FP$ ,  $TN$ ,  $FN$  denote true positive, false positive, true negative, and false negative, respectively.

To evaluate the performance of LVLMs in classifying objects with specific attributes when candidate categories are provided, we utilize an alternative accuracy measure ( $\mathcal{A}^*$ ), which quantifies the fraction of answers containing the correct category name. Given that the aforementioned models might produce similar but inconsistent categories for an object, the *semantic similarity* ( $\mathcal{S}$ ) used in vocabulary-free image classification [22] is additionally employed to quantify the similarity between predicted and ground-truth labels, irrespective of whether potential categories are provided (on *w/ vocabulary* and *w/o vocabulary*).

### 2.1.3 Benchmark Datasets

Our testbed draws upon a selection of salient object detection datasets, including DUTS [23] and SOC [15], along with specific datasets tailored for camouflaged object detection (COD10K [17]), transparent object detection (Trans10K [16]), polyp segmentation (ColonDB [20], ETIS [24], and CP-CHILD-B [25]), skin lesion detection (ISIC [19]), and anomaly detection (MVTec AD [21] and VisA [26]). Among these datasets, SOC, COD10K, CP-CHILD-B, MVTec AD,

and VisA contain both positive and negative samples (*i.e.*, images lacking specific objects), thereby constituting the data source for the full set, as previously mentioned. The positive sample proportions they possess are 0.500, 0.507, 0.250, 0.729, and 0.555, respectively. The remaining datasets that solely provide positive samples are utilized as the data source for the positive set. Moreover, COD10K, being the sole dataset that furnishes category labels for each object, is utilized for the classification of objects with specific attributes, yielding camouflaged object classification. Acknowledging the inherent challenge of discerning specific objects within negative samples, we solely utilize positive samples from COD10K for evaluation in this test.

### 2.1.4 Result Analyses and Discussions

The assessment outcomes for existence determination on both the full set and positive set, along with camouflaged object classification, are detailed in Table 1, Table 2, and Table 3. With the absence of negative samples in the positive set leading to  $TN = 0$  and  $FP = 0$ , the metric  $\mathcal{A}$  in Table 2 aligns directly with  $\mathcal{Y}$ . These findings reveal three key observations.

**Over-positive issue.** Based on the findings delineated in Table 1, each model attains a high score on metric  $\mathcal{Y}$ , wherein  $\mathcal{Y}$  denotes the proportion of the model yielding a positive response. Upon examination of the positive sample proportions within each dataset, as delineated in § 2.1.3, it becomes evident that these models consistently yield a greater frequency of positive responses compared to the actual proportion of positive samples. Especially concerning the SOC and CP-CHILD-B datasets, characterized by positive sample proportions of 0.5 and 0.25, the models’ positive response ratio exceeds 0.9. Regarding Table 2, where the metric  $\mathcal{A}$  corresponds directly to  $\mathcal{Y}$ , the notably high outcomes observed across various models in this table, particularly exemplified by LLaVA-1.5 achieving the result of 1.000 on multiple datasets, further support the notion that the models tend to generate positive responses. These observations suggest that the models are over-positive, which is consistent with recent works’ findings demonstrating a tendency for models to generate positive responses [27], [28].

**Limited performance in determining existence.** While achieving notably high accuracy ( $\mathcal{A}$ ) in Table 2, the inclusion of negative samples results in a deterioration of accuracy across the board, consistently dropping below 0.7 as depicted in Table 1. This diminished performance suggests an inadequate recognition of objects with specific attributes, particularly in the differentiation of negative samples. In these assessments, LLaVA-1.5 and Shikra showcase superior cognitive capabilities for camouflaged objects and anomalies, respectively, achieving higher accuracy ( $\mathcal{A}$ ) while maintaining a normal level on  $\mathcal{Y}$  in COD10K and MVTec AD/VisA. Furthermore, Shikra demonstrates relatively low results ( $\mathcal{Y}$ ) on COD10K due to its frequent misclassification of positive samples (consistently providing negative answers), indicating its significant challenge in recognizing camouflaged objects.

**Struggling with classifying camouflaged objects.** As illustrated in Table 3, when prompted to classify camouflaged objects with the provision of potential categories, LLaVA-1.5

TABLE 1

**Experimental results for three LVLMs regarding the presence of targets on full set.** We present the probability of positive answers ( $\mathcal{Y}$ , representing the percentage of “yes”). The highest accuracy ( $\mathcal{A}$ ) score is highlighted in **bold**.

| Model          | Natural scenes            |                           | Healthcare                | Industrial scenes         |                           |
|----------------|---------------------------|---------------------------|---------------------------|---------------------------|---------------------------|
|                | SOC [15]                  | COD10K [17]               | CP-CHILD-B [25]           | MVTec AD [21]             | VisA [26]                 |
|                | $\mathcal{A}/\mathcal{Y}$ | $\mathcal{A}/\mathcal{Y}$ | $\mathcal{A}/\mathcal{Y}$ | $\mathcal{A}/\mathcal{Y}$ | $\mathcal{A}/\mathcal{Y}$ |
| MiniGPT-v2 [4] | 0.513/0.987               | 0.580/0.909               | 0.250/0.990               | 0.695/0.874               | 0.543/0.875               |
| LLaVA-1.5 [12] | <b>0.618</b> /0.883       | <b>0.776</b> /0.427       | 0.268/0.983               | <b>0.750</b> /0.979       | 0.562/0.993               |
| Shikra [13]    | 0.528/0.973               | 0.535/0.053               | <b>0.285</b> /0.945       | 0.728/0.562               | <b>0.617</b> /0.251       |

TABLE 2

**Experimental results for three LVLMs regarding the presence of targets on positive set.** The highest accuracy score is marked in **bold**. Given the absence of negative samples in the positive set, resulting in  $TN = 0$  and  $FP = 0$ , the metric  $\mathcal{A}$  in this table is equivalent to  $\mathcal{Y}$ .

| Model          | Natural scenes |               | Healthcare    |               |               |
|----------------|----------------|---------------|---------------|---------------|---------------|
|                | DUTS [23]      | Trans10K [16] | ColonDB [20]  | ETIS [24]     | ISIC [19]     |
|                | $\mathcal{A}$  | $\mathcal{A}$ | $\mathcal{A}$ | $\mathcal{A}$ | $\mathcal{A}$ |
| MiniGPT-v2 [4] | 0.853          | 0.964         | 0.824         | 0.847         | 0.952         |
| LLaVA-1.5 [12] | 0.999          | <b>1.000</b>  | <b>1.000</b>  | <b>0.985</b>  | <b>1.000</b>  |
| Shikra [13]    | <b>1.000</b>   | 0.988         | 0.968         | 0.954         | 0.998         |

TABLE 3

**Quantitative results of three LVLMs on classifying camouflaged objects.** The best results are marked in **bold**. We conduct classification solely on the positive samples within this dataset.

| Setting               | Metric          | MiniGPT-v2 [4] | Shikra [13] | LLaVA-1.5 [12] |
|-----------------------|-----------------|----------------|-------------|----------------|
| <i>w/ vocabulary</i>  | $\mathcal{A}^*$ | 0.285          | 0.154       | <b>0.436</b>   |
| <i>w/ vocabulary</i>  | $\mathcal{S}$   | 0.567          | 0.545       | <b>0.673</b>   |
| <i>w/o vocabulary</i> | $\mathcal{S}$   | 0.607          | 0.608       | <b>0.655</b>   |

achieves an accuracy of 0.437 on metric  $\mathcal{A}^*$ , while Shikra only attains 0.154. These suboptimal outcomes could arise from various factors. Firstly, these models may face challenges in identifying camouflaged objects that closely resemble the background, as indicated by their unsatisfactory accuracy in Table 1. Secondly, the category of camouflaged objects may lie beyond the models’ domain of knowledge, hindering their ability to accurately match objects with their respective categories. Additionally, the extended length of the prompt, stemming from the incorporation of the camouflaged category, may impede the model’s comprehension. This observation aligns with the findings in Table 3, wherein the model demonstrates improved performance ( $\mathcal{S}$ ) when the candidate categories are excluded (*w/o vocabulary*), as opposed to when the vocabulary is provided (*w/ vocabulary*). In camouflaged object classification, LLaVA-1.5 demonstrates a stronger recognition capability compared to the other two models, as evidenced by achieving the best performance on all metrics under different settings in Table 3.

## 2.2 Uncovering Insights into Failure Cases

Recalling that these models encounter challenges in differentiating negative samples, we conduct tests on several negative samples to gain insight into the potential causes of this phenomenon. Models are prompted to provide additional descriptions or reasoning when determining the existence

of targets. We present the exploration of camouflaged attributes as examples and illustrate them in Fig. 2, where three potential factors are observed.

**Limited cognition towards specific attributes.** As illustrated in the first example of Fig. 2, when presented with the question “Is there camouflaged object in the picture? What is it?”, MiniGPT-v2 erroneously recognizes the “small black rock” as a camouflaged object, while LLaVA-1.5 also misclassifies a “plant” as such. These models classify objects belonging to the background, such as rocks and plants, as camouflaged objects simply because of their visual resemblance to the environment, suggesting their limited cognition towards camouflaged attributes.

**Object hallucinations.** Object hallucination, which involves generating objects in the description that are not present in the image [27], [29], could impact the recognition capability of LVLMs in specialized tasks. For instance, as demonstrated by the responses to the question “Is there camouflaged object in the picture? What is it?” in the second example of Fig. 2, where only the desert and the sky are visible, LLaVA-1.5 states that “a person is standing on the sandy beach”, while MiniGPT-v2 suggests that there is a “small bush or tree”. This phenomenon indicates that these models suffer from the issue of hallucination, which consequently results in the inaccurate perception of camouflaged objects [11].

**Text-to-image interference.** Based on our experimental findings, we infer that the models’ struggles in discriminating negative samples may also be attributed to text-to-image interference, which originates from the textual prompts supplied to the models [29]. As demonstrated in the second example, when prompted with “Please describe the picture in detail”, LLaVA-1.5 provides an accurate description of the image. However, when prompted with “Is there a camouflaged object in the picture? What is it?”, the mention of the “camouflaged object” in the prompt may interfere with the model’s generated description, resulting

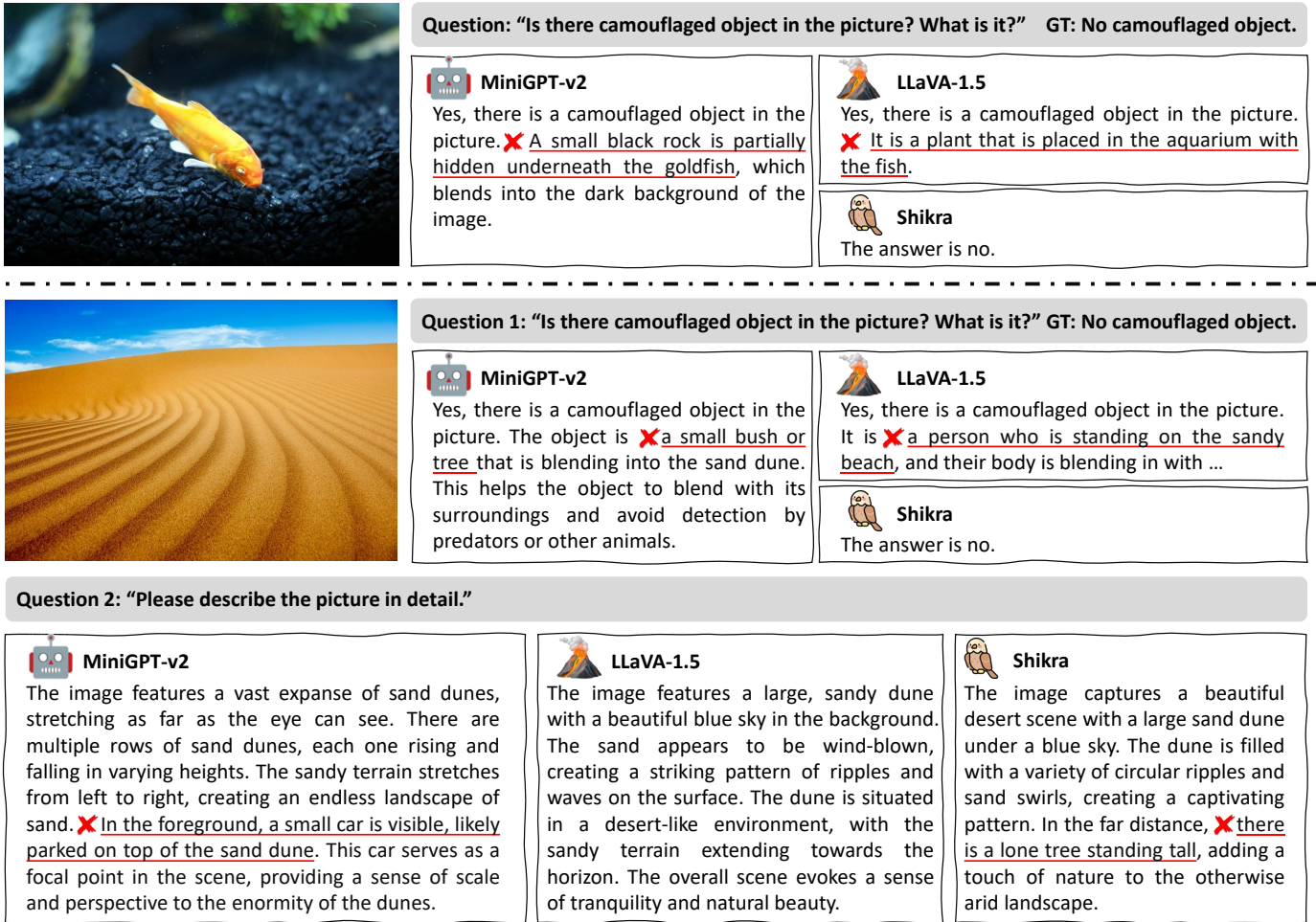


Fig. 2. Responses of three LVLMs regarding the perception of camouflaged objects on negative samples. Incorrect responses are underlined in red and marked with crosses.

in hallucinations and misjudgments by LLaVA-1.5.

## 2.3 Summary

This chapter evaluates the recognition capability of MiniGPT-v2 [4], LLaVA-1.5 [12], and Shikra [13] across various specialized tasks. Quantitative studies indicate that while these models exhibit certain cognitive abilities across various specialized tasks without domain-specific fine-tuning, their recognition performance requires further enhancement, particularly in differentiating negative samples. When directly applied to these tasks, they still demonstrate limited cognition and understanding of specialized domains. Apart from the limited cognition, other typical weaknesses of LVLMs, as revealed in qualitative investigations, such as object hallucinations, and text-to-image interference, likely lead to their insufficient performance in recognition tasks.

## 3 LOCALIZATION VIA LVLMS IN SPECIALIZED TASKS

In this chapter, we initially conduct a quantitative assessment of the models' localization capabilities. Furthermore, we delve deeper into their strengths and limitations by

validating their proficiency in localizing objects with specific attributes through the provision of additional descriptions.

## 3.1 Quantitative Investigation

### 3.1.1 Experimental Setup

Recent LVLMs demonstrate a remarkable visual grounding capability, enabling them to locate objects specified in language prompts (by providing the bounding box). This capability renders it feasible to apply these models to the specialized tasks described above. Indeed, the limitation of these models in providing only bounding boxes (bboxes) makes them challenging to directly apply to these segmentation tasks. Therefore, we adopt a two-step approach, consisting of detection followed by segmentation, to harness these models for the aforementioned specialized tasks. Concretely, as illustrated in Fig. 1, we initially prompt each model adaptively to provide bounding boxes for a particular type of object (e.g., transparent objects) with prompts like "Detect the <transparent objects>.", thus accomplishing the detection of the specific object. Subsequently, the predicted bounding boxes are used as prompts in the segment anything model (SAM) [30] to perform segmentation. Acknowledging that the ground-truth bounding box represents the desired target for LVLm detection in specialized tasks, we

TABLE 4

**Detection and segmentation results of MiniGPT-v2 [4], LLaVA-1.5 [12], and Shikra [13] on natural scenes.** The symbols  $\uparrow/\downarrow$  indicate that a higher/lower score is better, while the highest scores are marked in **bold**. The upper bound (on ground-truth bounding boxes) of detection and segmentation via LVLMs in diverse specialized tasks is marked in gray.

| Dataset       | Model          | Detection                   |                          |                      | Segmentation (with SAM applied to bboxes) |                                       |  |
|---------------|----------------|-----------------------------|--------------------------|----------------------|---|---------------------------------------|--|
|               |                | <i>Precision</i> $\uparrow$ | <i>Recall</i> $\uparrow$ | <i>F1</i> $\uparrow$ | <i>MAE</i> $\downarrow$                   | <i>F<math>\beta</math></i> $\uparrow$ | <i>S<math>\alpha</math></i> $\uparrow$ |
| DUTS [23]     | MiniGPT-v2 [4] | 0.296                       | <b>0.659</b>             | 0.409                | 0.195                                     | 0.580                                 | 0.662                                  |
|               | LLaVA-1.5 [12] | 0.270                       | 0.256                    | 0.263                | 0.458                                     | 0.241                                 | 0.347                                  |
|               | Shikra [13]    | <b>0.751</b>                | 0.583                    | <b>0.656</b>         | <b>0.102</b>                              | <b>0.711</b>                          | <b>0.754</b>                           |
|               | Upper bound    | 1.000                       | 1.000                    | 1.000                | 0.054                                     | 0.905                                 | 0.892                                  |
| SOC [15]      | MiniGPT-v2 [4] | 0.289                       | <b>0.464</b>             | <b>0.359</b>         | <b>0.197</b>                              | <b>0.446</b>                          | <b>0.578</b>                           |
|               | LLaVA-1.5 [12] | 0.155                       | 0.116                    | 0.133                | 0.388                                     | 0.245                                 | 0.314                                  |
|               | Shikra [13]    | <b>0.737</b>                | 0.013                    | 0.025                | 0.204                                     | 0.245                                 | 0.409                                  |
|               | Upper bound    | 1.000                       | 1.000                    | 1.000                | 0.027                                     | 0.956                                 | 0.932                                  |
| Trans10K [16] | MiniGPT-v2 [4] | 0.326                       | <b>0.355</b>             | 0.340                | 0.185                                     | 0.624                                 | 0.656                                  |
|               | LLaVA-1.5 [12] | 0.452                       | 0.250                    | 0.322                | 0.287                                     | 0.441                                 | 0.490                                  |
|               | Shikra [13]    | <b>0.614</b>                | 0.322                    | <b>0.431</b>         | <b>0.167</b>                              | <b>0.692</b>                          | <b>0.683</b>                           |
|               | Upper bound    | 1.000                       | 1.000                    | 1.000                | 0.108                                     | 0.868                                 | 0.824                                  |
| COD10K [17]   | MiniGPT-v2 [4] | <b>0.338</b>                | <b>0.575</b>             | <b>0.426</b>         | 0.308                                     | 0.390                                 | 0.524                                  |
|               | LLaVA-1.5 [12] | 0.284                       | 0.270                    | 0.277                | 0.454                                     | 0.226                                 | 0.352                                  |
|               | Shikra [13]    | 0.327                       | 0.301                    | 0.313                | <b>0.166</b>                              | <b>0.456</b>                          | <b>0.585</b>                           |
|               | Upper bound    | 1.000                       | 1.000                    | 1.000                | 0.054                                     | 0.808                                 | 0.844                                  |

employ it as the prompt for SAM to conduct segmentation. The segmentation results obtained in this manner serve as the upper bound. Taking into account the potential presence of multiple boxes in a picture, we employ SAM to perform segmentation with a single box as a hint. These results are then merged using Boolean OR operation to derive the final segmentation result. The SAM version with ViT-H [31] as default backbone is employed in all experiments to ensure a fair comparison across the board.

### 3.1.2 Metrics

As mentioned previously, we initially perform detection followed by segmentation to utilize these models for specialized tasks. Therefore, during evaluation, we assess their localization abilities by evaluating their performance in both detection and segmentation. To evaluate the detection results, three widely used detection metrics (*i.e.*, *Precision*, *Recall*, and *F1* with an intersection over union (IoU) threshold of 0.5 [32]) are adopted. Additionally, three segmentation metrics (mean absolute error (*M*) [33], S-measure (*S $\alpha$* ) [34], and maximum F-measure (*F $\beta$* ) [35]) are employed to assess segmentation performance. It should be noted that since these models solely predict bounding boxes without providing corresponding confidence values, we exclude the adoption of commonly used metrics like mean average precision (*mAP*) [32] in object/anomaly detection.

### 3.1.3 Benchmark Datasets

The datasets mentioned in § 2.1, with the exception of CP-CHILD-B [25] that only annotates the presence of polyps, are utilized to evaluate the localization capability. These datasets are tailored for segmentation tasks, thus providing only the corresponding mask annotations. To evaluate the detection performance, we derive ground truth bounding boxes from masks. Taking into account the inherent difficulty of recognizing specific objects on negative samples, as demonstrated in § 2, we solely utilize positive samples from the aforementioned datasets to assess the localization capability.

### 3.1.4 Result Analyses and Discussions

The detection and segmentation results are presented in Table 4-6. Several noteworthy observations can be gleaned from these findings.

**Promising yet insufficient localization capability for specific tasks.** The outcomes presented in Table 4-6 suggest that MiniGPT-v2 [4], LLaVA-1.5 [12], and Shikra [13] hold promise in addressing specialized tasks without requiring domain-specific fine-tuning, particularly in natural scenes. For example, Shikra demonstrates superior segmentation performance on datasets like DUTS (*S $\alpha$*  score: 0.754) and Trans10K (*S $\alpha$*  score: 0.683), even when provided only with category names. Among these models, Shikra and MiniGPT-v2 showcase superior localization ability in these tasks compared to LLaVA-1.5. Among these models, Shikra and MiniGPT-v2 exhibit superior localization ability in these tasks compared to LLaVA-1.5. While these models exhibit some potential for addressing specialized tasks, their detection and segmentation performance is found to be inadequate, suggesting insufficient localization capability in specialized tasks. The low scores in terms of *Precision*, *Recall*, and *F1* demonstrate that these models struggle with precise bounding box generation (with most predicted bounding boxes being inaccurate) and accurate identification of targets (cannot accurately provide bounding boxes for most objects). These limitations further restrict the final segmentation performance on specialized tasks.

**Superior performance in natural scenarios.** According to the results presented in Table 4-6, these models demonstrate superior performance in natural scenarios, especially on DUTS and Trans10K. The underlying reason may be that transparent and salient objects are more prevalent, exhibiting common attributes. Conversely, medical and abnormal images are relatively scarce and possess complex characteristics, thereby reducing the generalization capability of LVLMs.

Additionally, we illustrate the detection and segmentation results in Fig. 3. As evident, these models face challenges in accurately providing the bounding box, con-

TABLE 5

**Detection and segmentation results of MiniGPT-v2 [4], LLaVA-1.5 [12], and Shikra [13] on healthcare.** The symbols  $\uparrow/\downarrow$  indicate that a higher/lower score is better, while the highest scores are marked in **bold**. The upper bound (on ground-truth bounding boxes) of detection and segmentation via LVLMs in diverse specialized tasks is marked in gray.

| Dataset      | Model          | Detection                   |                          |                      | Segmentation (with SAM applied to bboxes) |  |   |
|--------------|----------------|-----------------------------|--------------------------|----------------------|---|--|---|
|              |                | <i>Precision</i> $\uparrow$ | <i>Recall</i> $\uparrow$ | <i>F1</i> $\uparrow$ | <i>MAE</i> $\downarrow$                   | <i>F<math>_{\beta}</math></i> $\uparrow$ | <i>S<math>_{\alpha}</math></i> $\uparrow$ |
| ColonDB [20] | MiniGPT-v2 [4] | 0.153                       | <b>0.287</b>             | 0.199                | 0.322                                     | <b>0.281</b>                             | 0.467                                     |
|              | LLaVA-1.5 [12] | <b>0.245</b>                | 0.237                    | <b>0.241</b>         | <b>0.190</b>                              | 0.273                                    | <b>0.504</b>                              |
|              | Shikra [13]    | 0.163                       | 0.163                    | 0.163                | 0.540                                     | 0.232                                    | 0.338                                     |
|              | Upper bound    | 1.000                       | 1.000                    | 1.000                | 0.019                                     | 0.906                                    | 0.916                                     |
| ETIS [24]    | MiniGPT-v2 [4] | 0.116                       | <b>0.221</b>             | <b>0.152</b>         | <b>0.523</b>                              | 0.196                                    | <b>0.336</b>                              |
|              | LLaVA-1.5 [12] | 0.092                       | 0.087                    | 0.089                | 0.640                                     | 0.197                                    | 0.268                                     |
|              | Shikra [13]    | <b>0.148</b>                | 0.139                    | 0.144                | 0.675                                     | <b>0.206</b>                             | 0.261                                     |
|              | Upper bound    | 1.000                       | 1.000                    | 1.000                | 0.006                                     | 0.912                                    | 0.947                                     |
| ISIC [19]    | MiniGPT-v2 [4] | 0.321                       | <b>0.610</b>             | 0.421                | 0.350                                     | <b>0.561</b>                             | <b>0.509</b>                              |
|              | LLaVA-1.5 [12] | <b>0.573</b>                | 0.568                    | <b>0.570</b>         | 0.404                                     | 0.519                                    | 0.442                                     |
|              | Shikra [13]    | 0.398                       | 0.398                    | 0.398                | <b>0.348</b>                              | 0.430                                    | 0.448                                     |
|              | Upper bound    | 1.000                       | 1.000                    | 1.000                | 0.106                                     | 0.842                                    | 0.765                                     |

TABLE 6

**Detection and segmentation results of MiniGPT-v2 [4], LLaVA-1.5 [12], and Shikra [13] on industrial scenes.** The symbols  $\uparrow/\downarrow$  indicate that a higher/lower score is better, while the highest scores are marked in **bold**. The upper bound (on ground-truth bounding boxes) of detection and segmentation via LVLMs in diverse specialized tasks is marked in gray.

| Dataset       | Model          | Detection                   |                          |                      | Segmentation (with SAM applied to bboxes) |  |   |
|---------------|----------------|-----------------------------|--------------------------|----------------------|---|--|---|
|               |                | <i>Precision</i> $\uparrow$ | <i>Recall</i> $\uparrow$ | <i>F1</i> $\uparrow$ | <i>MAE</i> $\downarrow$                   | <i>F<math>_{\beta}</math></i> $\uparrow$ | <i>S<math>_{\alpha}</math></i> $\uparrow$ |
| MVTec AD [21] | MiniGPT-v2 [4] | 0.107                       | 0.212                    | 0.142                | 0.511                                     | 0.381                                    | 0.292                                     |
|               | LLaVA-1.5 [12] | 0.081                       | 0.065                    | 0.072                | 0.580                                     | 0.061                                    | 0.239                                     |
|               | Shikra [13]    | <b>0.355</b>                | <b>0.281</b>             | <b>0.314</b>         | <b>0.090</b>                              | <b>0.425</b>                             | <b>0.622</b>                              |
|               | Upper bound    | 1.000                       | 1.000                    | 1.000                | 0.032                                     | 0.784                                    | 0.831                                     |
| VisA [26]     | MiniGPT-v2 [4] | 0.009                       | 0.032                    | 0.014                | 0.211                                     | 0.051                                    | 0.410                                     |
|               | LLaVA-1.5 [12] | 0.007                       | 0.007                    | 0.007                | 0.532                                     | 0.016                                    | 0.259                                     |
|               | Shikra [13]    | <b>0.107</b>                | <b>0.076</b>             | <b>0.089</b>         | <b>0.100</b>                              | <b>0.153</b>                             | <b>0.505</b>                              |
|               | Upper bound    | 1.000                       | 1.000                    | 1.000                | 0.004                                     | 0.697                                    | 0.819                                     |

sequently resulting in subpar segmentation performance. These findings underscore their limited localization capability in specialized tasks.

### 3.2 Uncovering Insights into Failure Cases

As mentioned in § 3.1, we assess the localization capability of recent LVLMs in specialized tasks solely by providing category names. This setting concurrently evaluates the models’ recognition, reasoning, and localization capabilities by requiring models to accurately perceive each object, determine targets through reasoning, and ultimately precisely locate them. Therefore, we sought to gain insight into the underlying reasons behind the inability to locate specific objects by breaking down the above task into multiple parts. Specifically, in natural scenarios involving salient/transparent/camouflaged objects, as illustrated in Fig. 4, two questions are prompted to assess the abilities of the models in accurately localizing given objects (“Question 1”) and determining the target with specific attributes (“Question 2”). In industrial scenarios, we examine the models’ recognition of anomalies by querying the existence (“Question 1”) and image description (“Question 2”), and further test their ability to locate anomalous areas by providing corresponding descriptions “Question 3”), as depicted in Fig. 5. Another test on healthcare (colon polyp detection), following the same protocol as in industrial scenarios, is also conducted, and the results are presented in Fig. 6. Two

underlying reasons behind the inability to locate specific objects can be inferred from the above experiments.

**Decreased robustness in complex problems.** Indeed, combining the findings from Fig. 3 and Fig. 4 reveals that these models excel when tasked with locating a given object or inferring the target. However, they encounter difficulties when directly tasked with locating the target. This phenomenon indicates that though these models demonstrate proficient reasoning and localization capabilities, they exhibit decreased robustness or are unskilled when faced with more complex problems. Moreover, it is observed that the recognition of camouflaged objects poses a challenge for these models in comparison to salient objects and transparent entities. This observed difficulty may be attributed to the inherent resemblance of camouflaged objects to their ambient surroundings, consequently impacting the effectiveness of LVLMs in tasks pertaining to recognition and detection. The misclassification exhibited by the aforementioned models accentuates the intricate nature of accurately associating camouflaged objects with their designated categories, as mentioned in § 2.2.

**Limited cognition toward medical images and anomalies.** Another observation pertains to the models’ restricted cognitive capacity in processing medical images and anomalies, exemplified by instances such as LLaVA-1.5 and Shikra erroneously categorizing the “black and orange color scheme” and “the number 500” as anomalies (as addressed

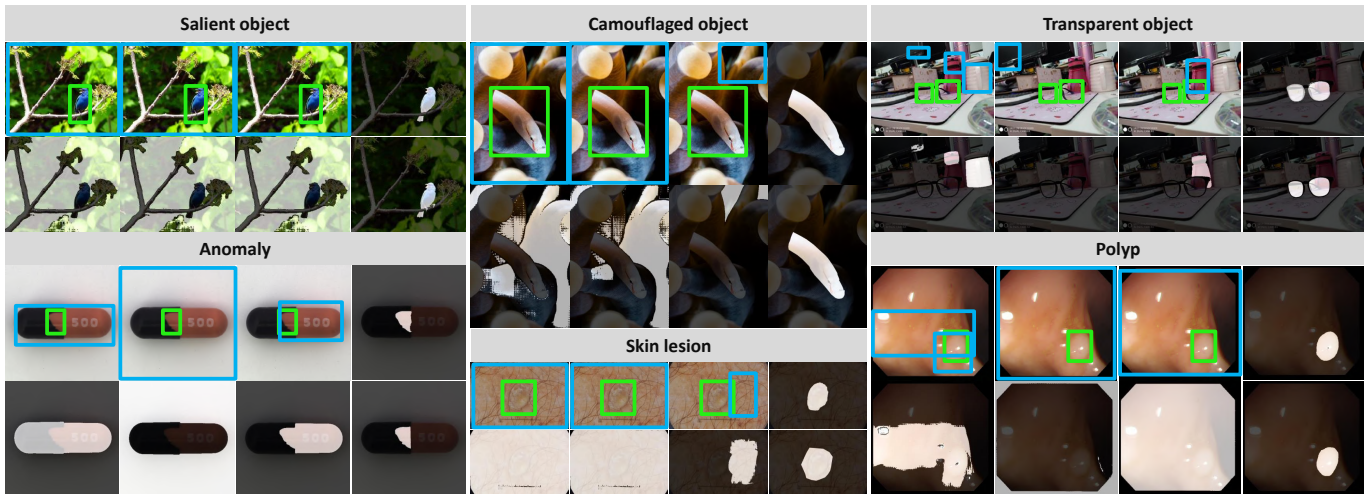


Fig. 3. Detection and segmentation results of three LVLMs across six specialized tasks. The predicted bounding box and ground-truth are marked with blue and green. From left to right in each scene: detection (top) and segmentation (bottom) results of MiniGPT-v2, LLaVA-1.5, and Shikra, as well as segmentation results with GT-BBOX (top) and ground-truth masks (bottom).

in “Question 1” within Fig. 5). Additionally, MiniGPT-v2 exhibited a misclassification by identifying the colon image as “the inside of an orange” (as indicated in “Question 2” within Fig. 6). It is noteworthy to highlight the superior localization capabilities demonstrated by these models in polyp segmentation tasks when provided with pertinent descriptions (as evidenced in responses to “Question 3”); nevertheless, there remains scope for enhancement in their performance regarding anomaly detection.

### 3.3 Summary

This chapter evaluates the effectiveness of MiniGPT-v2 [4], LLaVA-1.5 [12], and Shikra [13] in accurately localizing specific objects across diverse specialized tasks. The outcomes suggest that these models hold promise in addressing specialized tasks (particularly in natural scenes), while Shikra and MiniGPT-v2 showcase superior localization ability compared to LLaVA-1.5. Nonetheless, despite showcasing promise, the detection and segmentation performance of these models are deemed inadequate, indicating a shortfall in localization capability for specialized tasks. The observed limited cognition towards medical images and anomalies hampers the generalization ability of these models, while decreased robustness when faced with complex problems may serve as an additional constraint on the localization capability.

## 4 CAPABILITIES OF LVLMS IN GENERAL TASKS

The chapters outlined above offer a comprehensive evaluation of three recent open-source LVLMs, effectively illustrating their shortcomings in both recognition and localization capabilities when applied to specialized tasks. In this chapter, we undertake empirical investigations to offer insight into the performance of MiniGPT-v2 [4], LLaVA-1.5 [12], Shikra [13], as well as GPT-4V [5] across a range of general tasks. Given that the recognition and localization of common objects serve as optimization objectives for many current LVLMs and their performance on these problems

has been extensively studied [4], [12], [13], we shift our focus to five other widely recognized comprehensive general tasks to evaluate their general capabilities. Capabilities to be evaluated in this investigation encompass object counting, absurd question answering, affordance reasoning, attribute recognition, and spatial relation reasoning. We opt to utilize three natural scenes sourced from the COCO [14] dataset to empirically validate their performance across general tasks. The outcomes of these assessments are visually depicted in Fig. 7, Fig. 8, and Fig. 9.

### 4.1 Object Counting

A proficient object counting ability serves as a testament to the comprehensive performance of LVLMs. This capability necessitates the model’s capacity not only to differentiate and recognize individual objects but also to possess a robust numerical comprehension within a visual context. To empirically evaluate the object counting ability, we employ prompts such as “How many...” across three scenes in Fig. 7-9. The outcomes reveal that MiniGPT-v2, LLaVA-1.5, and Shikra achieve only one-third accuracy on this question, whereas GPT-4V fails on all scenes. This underscores the substantial room for enhancement in the counting ability of LVLMs. Moreover, the inability and inefficacy of these models in counting challenging objects, including small objects (Fig. 8), serve to underscore the imperative of enhancing the visual perception capabilities inherent in vision models.

### 4.2 Absurd Question Answering

Recent LVLMs demonstrate the capacity to seamlessly integrate both textual and visual inputs, thereby forging intricate associations between textual attributes and visual characteristics. However, an intriguing question arises: what transpires when there exists a lack of compatibility between the textual content and the accompanying image? To interrogate this phenomenon, we endeavor to subject these models to absurd inquiries within assessments. As delineated in Fig. 7-9, our investigation entailed posing the question,



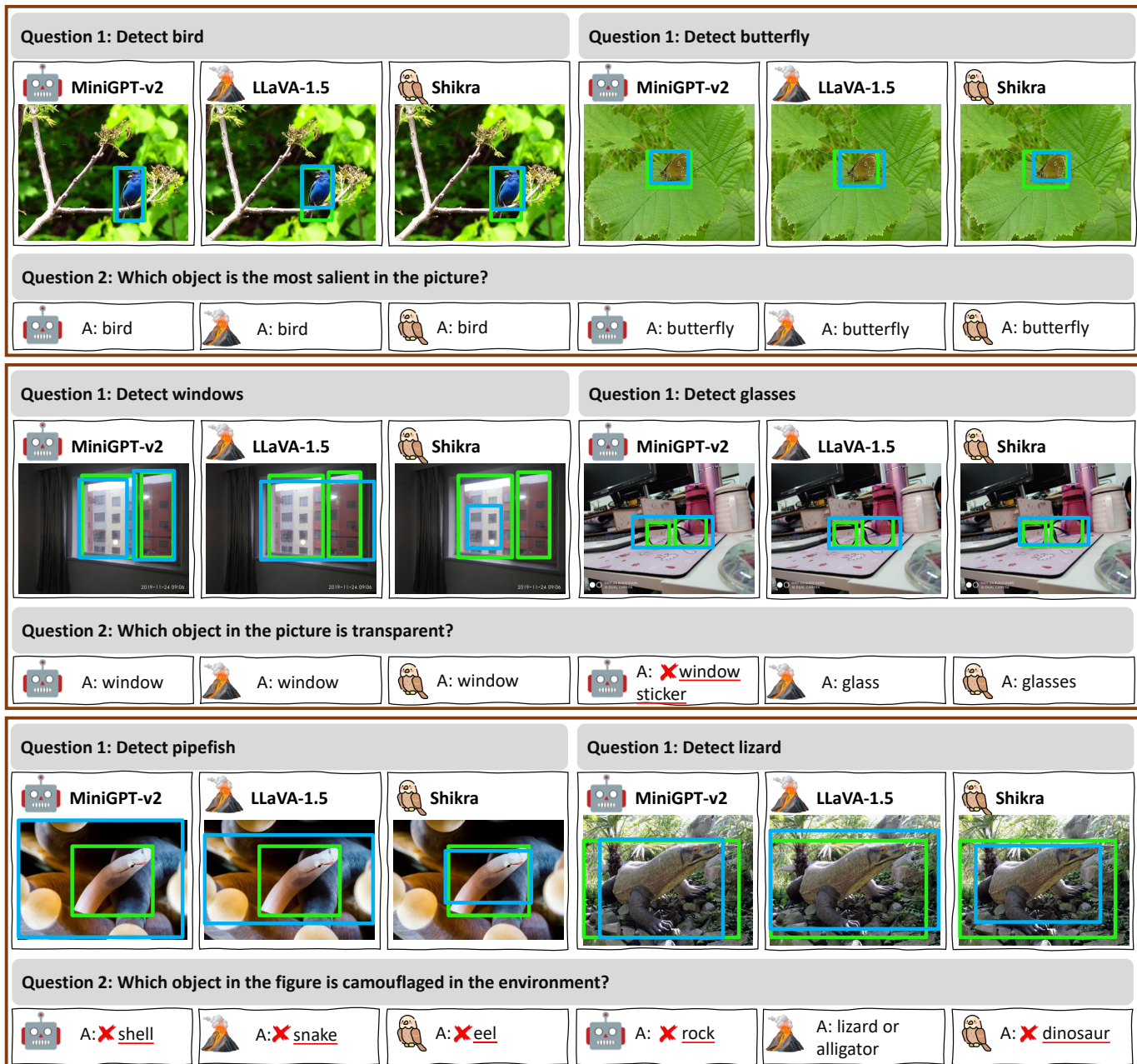


Fig. 4. Responses of three LLMs regarding locating given objects and recognizing objects with specific attributes. Predicted bounding boxes and ground-truth are marked in blue and green. From top to bottom: examples of salient object detection, transparent object detection, and camouflaged object detection. Incorrect responses are marked in red underlines and crosses.

“What color is the airplane in the picture?”, across three distinct scenes devoid of any airplane presence. Remarkably, our findings unveil a consistent trend: while the majority of models yielded precise color descriptions of the non-existent airplane, notably, GPT-4V diverged in its response. This empirical observation underscores the nuanced discrepancy between visual and language information processing within these models, thereby illuminating potential disparities in their semantic understanding. Specifically, the language input appears to imbue the model with prior information, potentially leading to erroneous judgments or text-to-image interference—a phenomenon referred to as hallucination [29]. An intriguing observation worthy of mention is the robust capability demonstrated by GPT-4V in navigating absurd inquiries, as it consistently provides the answer “no airplane”

for all three scenarios.

### 4.3 Affordance Reasoning

Affordance delineates the cognitive grasp of models regarding the potential functionalities or interactions that an object can offer [7]. Our study delves into affordance assessments across three scenarios, employing inquiries such as “What objects in the picture can I ...”. The outcomes evince skilled performance of the models in this assessment, adeptly identifying objects capable of executing the prescribed actions. These findings substantiate the models’ robust comprehension of object functionality, elucidating their adeptness in establishing associations between actions and corresponding objects.

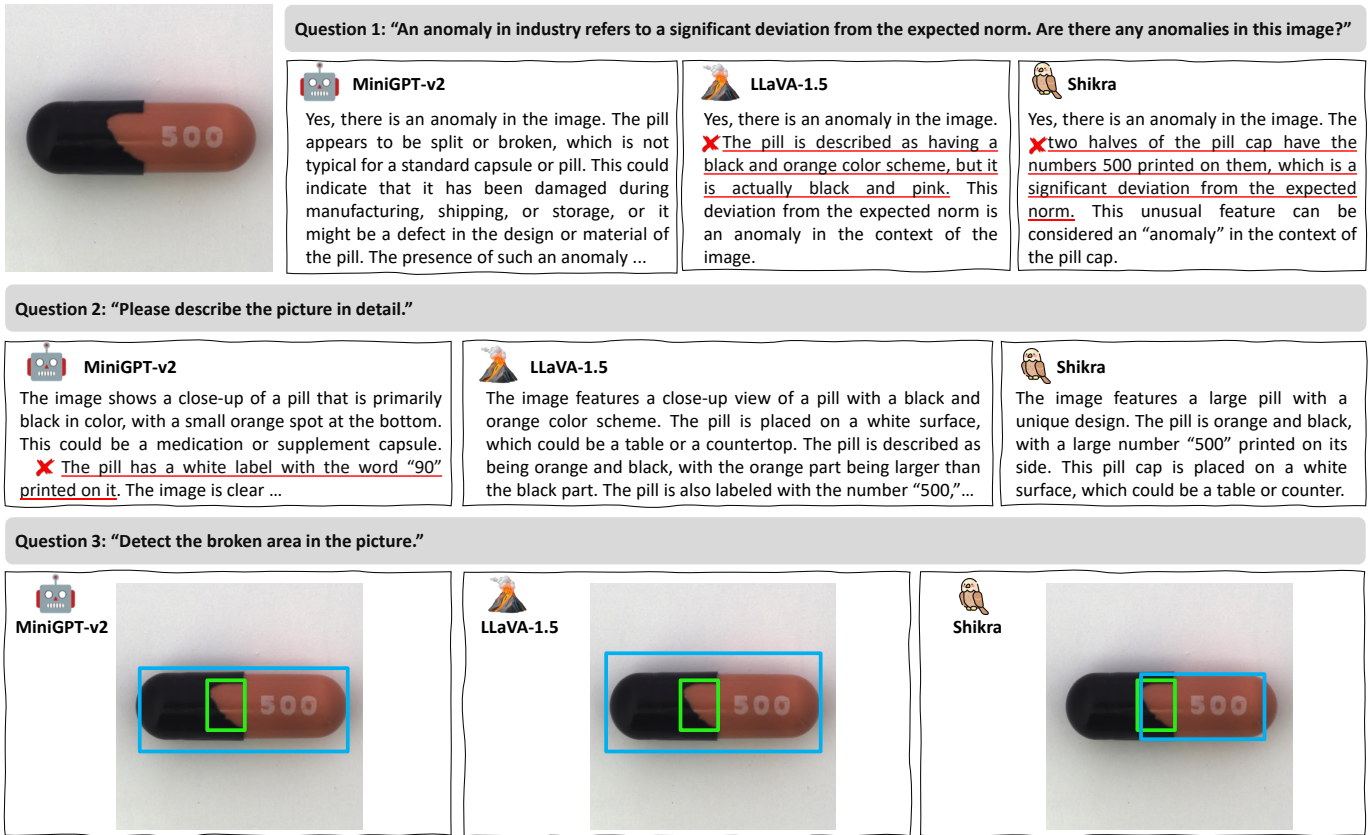


Fig. 5. Responses of three LVLMs regarding recognizing and locating the anomaly. Predicted bounding boxes and ground-truth are marked in blue and green, respectively. The incorrect responses are marked in red underlines and crosses.

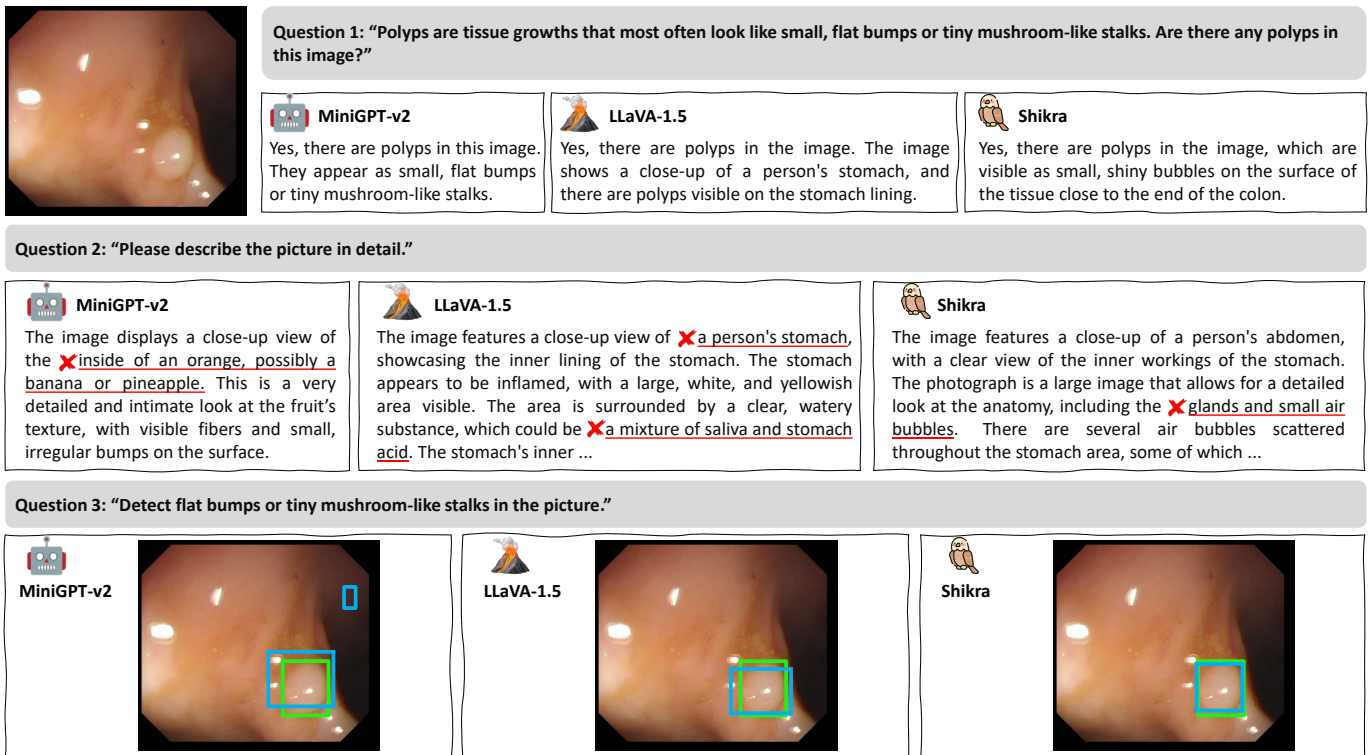







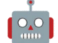



Fig. 6. Responses of three LVLMs regarding recognizing and locating the colon polyp. Predicted bounding boxes and ground-truth are marked in blue and green, respectively. Incorrect responses are marked in red underlines and crosses.



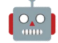



**Question 1: "How many pandas are there in the picture?"** GT: 2.

|  |  |
|--|--|
|  <b>MiniGPT-v2</b><br>✗ <u>1</u>                          |  <b>Shikra</b><br>The answer is 2.                                      |
|  <b>LLaVA-1.5</b><br>There are two pandas in the picture. |  <b>GPT-4V</b><br>✗ <u>I'm sorry, I can't assist with that request.</u> |





**Question 2: "What color is the airplane in the picture?"** GT: No airplane.

|  |  |  |  |
|--|--|--|--|
|  <b>MiniGPT-v2</b><br>✗ <u>White.</u> |  <b>Shikra</b><br>✗ <u>The answer is white.</u> |  <b>LLaVA-1.5</b><br>✗ <u>The airplane in the picture is red.</u> |  <b>GPT-4V</b><br>Sorry, I can't provide information about that image as there's no airplane visible in it. |
|--|--|--|--|

**Question 3: "What objects in the picture can I sit on?"** GT: Chair.

|  |  |  |   |
|--|--|--|---|
|  <b>MiniGPT-v2</b><br>Chairs. |  <b>Shikra</b><br>The answer is chairs. |  <b>LLaVA-1.5</b><br>In the picture, there are chairs available for people to sit on. |  <b>GPT-4V</b><br>In the picture, you can sit on the chairs that are around the table. |
|--|--|--|---|

**Question 4: "What colors are the flowers in the picture?"** GT: Red and yellow.

|   |  |  |   |
|---|--|--|---|
|  <b>MiniGPT-v2</b><br>✗ <u>Yellow.</u> |  <b>Shikra</b><br>The answer is red and yellow. |  <b>LLaVA-1.5</b><br>The flowers in the picture are red and yellow. |  <b>GPT-4V</b><br>The flowers in the picture are primarily red and yellow. There appear to be some green leaves among the flowers as well. |
|---|--|--|---|

**Question 5: "Which of the three women in the picture is closest to the orange juice?"** GT: The woman in colorful stripes or left.





|  |  |   |   |
|--|--|---|---|
|  <b>MiniGPT-v2</b><br>✗ <u>Right.</u> |  <b>Shikra</b><br>The answer is left. |  <b>LLaVA-1.5</b><br>The ✗ <u>woman in the black suit</u> is sitting next to the orange juice. |  <b>GPT-4V</b><br>In the image, the woman on the left, wearing a striped top, is closest to the orange juice. The glass of orange juice is located on the table to her immediate left. |
|--|--|---|---|

Fig. 7. Responses of four LVLMs (MiniGPT-v2, LLaVA-1.5, Shikra, and GPT-4V) regarding five general tasks, encompassing object counting (question 1), absurd question answering (question 2), affordance reasoning (question 3), attribute recognition (question 4), and spatial relation reasoning (question 5). Incorrect responses are marked in red underlines and crosses.

#### 4.4 Attribute Recognition

We proceed to validate the object attribute recognition capabilities of the aforementioned models through the utilization of "question4", as delineated in Fig. 7-9. With the exception of MiniGPT-v2 in the first scenario, all other models exhibit commendable attribute-aware performance. The results suggest that there is a greater need for improvement in MiniGPT-v2 compared to the other models.

#### 4.5 Spatial Relation Reasoning

Comprehending the spatial relationships between objects entails a multifaceted task. Achieving accurate understanding of these positional mandates the possession of object recognition, object localization, and reasoning abilities within the model's architecture. In this context, we evaluate the models' spatial relation reasoning ability by analyzing their responses to the final question in Fig. 7-9. As evident, the error rate for these inquiries is elevated. Specifically, in the first scenario, both MiniGPT-v2 and LLaVA-1.5 yield inaccurate responses. In the second scenario, erroneous answers are provided by GPT-4V and LLaVA-1.5. Conversely, in the third scenario, only the response from MiniGPT-v2

proves correct. While demonstrating adeptness in object recognition, these models reveal a deficiency in localization and spatial reasoning capabilities, highlighting the necessity for further refinement in these areas.

## 5 CONCLUSION

### 5.1 Concluding Remarks

In this study, we assess the progress of LVLMs by evaluating their effectiveness across specialized and general tasks. We begin by evaluating the performance of three recent open-source LVLMs – MiniGPT-v2, LLaVA-1.5, and Shikra – using a comprehensive testbed comprising three distinct scenarios (natural, healthcare, and industrial) alongside six specialized tasks. These tasks include salient, camouflaged, and transparent object detection, as well as polyp and skin lesion detection, alongside industrial anomaly detection. Additional empirical investigations are conducted on GPT-4V and the aforementioned models to assess their capabilities across general tasks. The quantitative findings indicate that while these models demonstrate promise in specialized tasks, they manifest inadequate generalization, particularly in recognition and localization, when directly applied to













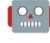







|   |   |  |  |
|---|---|--|--|
|                                | Question 1: "How many scattered cigarettes are there in the picture?"   |  | GT: 3.   |
|   |  MiniGPT-v2<br>❌ <u>4</u>                |  Shikra<br>❌ <u>The answer is 2.</u>                       |  LLaVA-1.5<br>❌ <u>There are two scattered cigarettes in the picture.</u>   |
| Question 2: "What color is the airplane in the picture?"  |   |  |  |
| GT: No airplane.  |   |  |  |
|  MiniGPT-v2<br>❌ <u>White.</u> |  Shikra<br>❌ <u>The answer is white.</u> |  LLaVA-1.5<br>❌ <u>The airplane in the picture is red.</u>  |  GPT-4V<br>I'm sorry, but there seems to be a misunderstanding. The picture you've shared does not contain an airplane. It features ...   |
| Question 3: "Where can I sit?"  |   |  |  |
| GT: Chair.  |   |  |  |
|  MiniGPT-v2<br>❌ <u>Floor.</u> |  Shikra<br>The answer is chair.          |  LLaVA-1.5<br>You can sit on a chair in the room.           |  GPT-4V<br>This image shows ..., ❌ <u>there are no actual seats available in the image. If you need to sit, you would need to find a chair or a seating area not visible in this image.</u> |
| Question 4: "What color is the chair in the picture?"   |   |  |  |
| GT: Red.  |   |  |  |
|  MiniGPT-v2<br>Red.            |  Shikra<br>The answer is red.            |  LLaVA-1.5<br>The chair in the picture is red.              |  GPT-4V<br>The chair in the picture is red.   |
| Question 5: "In the picture, which is closer to the chair, the cigarette or the bottle?"                        |   |  |  |
| GT: Cigarette.  |   |  |  |
|  MiniGPT-v2<br>Cigarette.    |  Shikra<br>The answer is cigarette.    |  LLaVA-1.5<br>❌ <u>The bottle is closer to the chair.</u> |  GPT-4V<br>In the image, ❌ <u>the bottle appears to be closer to the chair</u> compared to the cigarette pack...  |

Fig. 8. Responses of four LVLMs (MiniGPT-v2, LLaVA-1.5, Shikra, and GPT-4V) regarding five general tasks, encompassing object counting (question 1), absurd question answering (question 2), affordance reasoning (question 3), attribute recognition (question 4), and spatial relation reasoning (question 5). Incorrect responses are marked in red underlines and crosses.

these tasks. This limitation stems from their constrained understanding of specialized task domains. In addition to the aforementioned limitation, performance challenges are exacerbated by typical weaknesses observed in LVLMs. These include issues such as object hallucination, text-to-image interference, and decreased robustness when confronted with complex problem-solving scenarios. In addition to the lack of generalization in specialized tasks, the subpar performance of LVLMs in tasks such as object counting, spatial relation reasoning, and absurd question answering underscores their limited proficiency in generic tasks as well. The inadequacies observed in both specialized and general tasks highlight a significant gap that LVLMs have yet to bridge on the path towards achieving artificial general intelligence.

## 5.2 Discussions

Based on the findings presented, we initiate several discussions concerning the advanced application of LVLMs in specialized tasks and their future development. We anticipate that our discussion could ignite thinking among readers and facilitate further exploration in this field.

**Exploring more effective prompts.** While recent LVLMs demonstrate some usability for various specialized tasks, they face hurdles in directly extrapolating to specialized tasks without fine-tuning and training, particularly when tasked with discerning the presence or localization of a target solely based on keywords or task names. Providing additional context within prompts has been shown to enhance their performance, as demonstrated in our investigation and some recent studies, which adopted strategies such as offering more detailed anomaly definitions in prompts while providing expected question-answering examples [10], and incorporating additional features of camouflaged targets into the prompts [11]. Therefore, exploring more effective prompts customized for each specialized task, a practice known as prompt engineering [36], emerges as a viable strategy for bolstering the performance of LVLMs in specific tasks.

**Optimizing LVLMs toward specialized tasks.** Despite being trained on extensive datasets that enable LVLMs to recognize common objects effectively, their deficiency in specific domain knowledge poses a significant obstacle to their efficacy in specialized tasks [8]. As previously

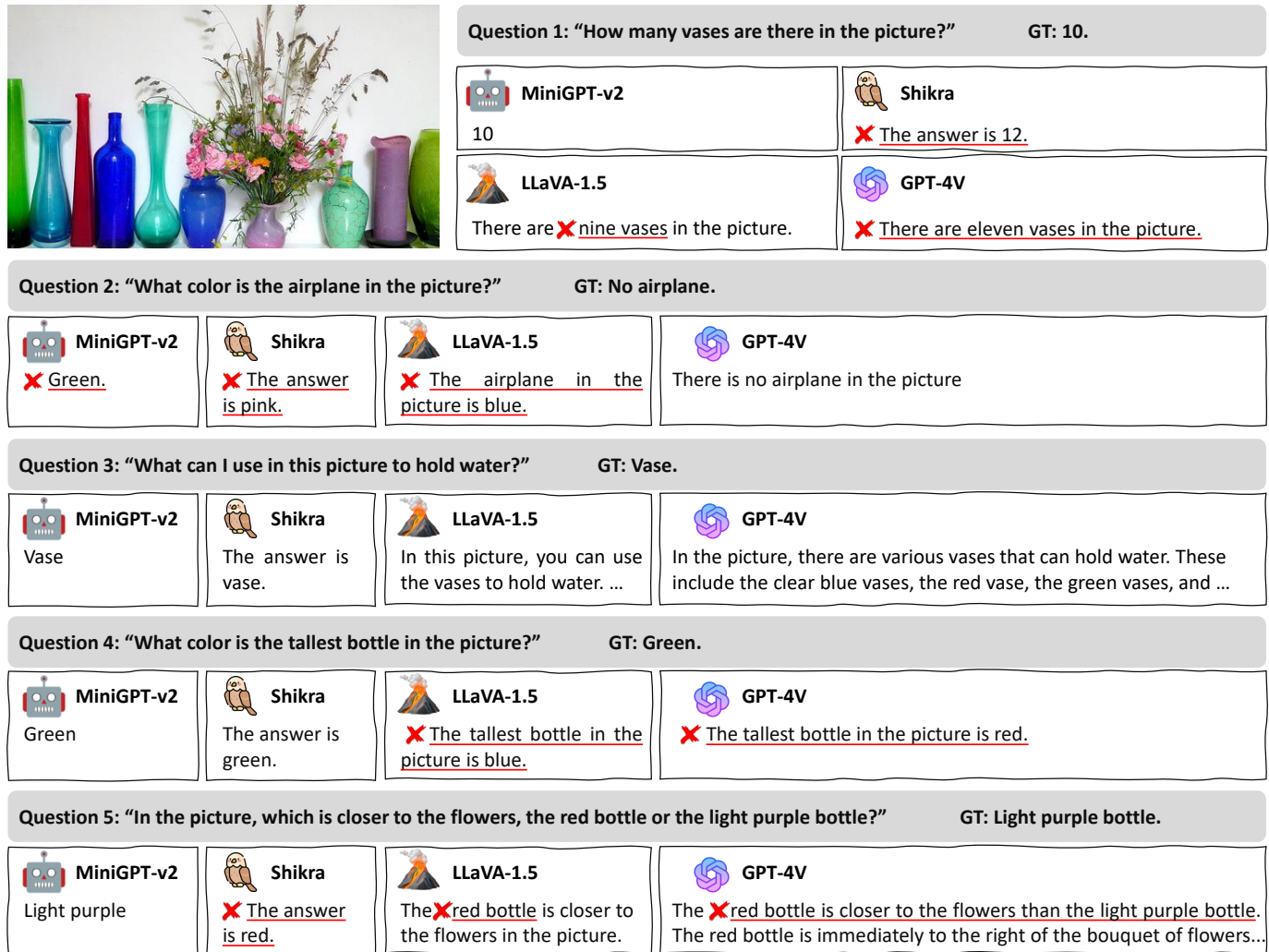


Fig. 9. Responses of four LVMs (MiniGPT-v2, LLaVA-1.5, Shikra, and GPT-4V) regarding five general tasks, encompassing object counting (question 1), absurd question answering (question 2), affordance reasoning (question 3), attribute recognition (question 4), and spatial relation reasoning (question 5). Incorrect responses are marked in red underlines and crosses.

noted, prompt engineering has shown promise in enhancing LVM performance on certain tasks. However, for certain tasks, particularly those with target characteristics that are challenging to describe clearly, such as camouflaged object detection and anomaly detection, the efficacy of prompt engineering is limited. Hence, one of the future research directions involves optimizing LVMs for specific tasks. This can be achieved by incorporating domain-specific knowledge through techniques such as prompt-tuning or fine-tuning [8], [37], thereby enhancing their performance in specialized tasks.

**Mitigating hallucination and also other issues.** Current LVMs encounter significant challenges related to hallucination such as object hallucination and image-to-text interference [27], [29], [38], [39], which impact their efficacy across both general and specific tasks. In future research endeavors, overcoming these challenges by leveraging techniques such as hallucination revisor [38] and chain of visual perception [11] holds promise for enhancing the efficacy of LVMs across diverse tasks and facilitating broader application of these models in practical settings. Besides, it is equally imperative to implement suitable strategies, such as data augmentation that eliminate co-occurrence pat-

terns [40], to address the underlying issues of LVMs. Apart from the hallucination problem, these models encounter additional challenges, including decreased robustness when confronted with complex problems and reduced effectiveness in numerous general tasks, which underscore the fact that the comprehensive capabilities of current LVMs remain constrained. Future research is anticipated to leverage increasingly challenging datasets/problems while also providing detailed and specific procedures in instruction tuning [13], [41] to enhance the comprehensive capabilities of LVMs. Besides, adopting advanced techniques like feedback/reward mechanisms [42], [43] and integrating expert models [44] are also viable avenues to enhance their capabilities.

## REFERENCES

- [1] T. Brown, B. Mann, N. Ryder, M. Subbiah, J. D. Kaplan, P. Dhariwal, A. Neelakantan, P. Shyam, G. Sastry, A. Askell, S. Agarwal, A. Herbert-Voss, G. Krueger, T. Henighan, R. Child, A. Ramesh, D. Ziegler, J. Wu, C. Winter, C. Hesse, M. Chen, E. Sigler, M. Litwin, S. Gray, B. Chess, J. Clark, C. Berner, S. McCandlish, A. Radford, I. Sutskever, and D. Amodei, "Language models are few-shot learners," in *Advances in Neural Information Processing Systems*, 2020, pp. 1877–1901.

- [2] H. Touvron, T. Lavril, G. Izacard, X. Martinet, M.-A. Lachaux, T. Lacroix, B. Rozière, N. Goyal, E. Hambro, F. Azhar *et al.*, “Llama: Open and efficient foundation language models,” *arXiv preprint arXiv:2302.13971*, 2023.
- [3] H. Liu, C. Li, Q. Wu, and Y. J. Lee, “Visual instruction tuning,” in *Advances in Neural Information Processing Systems*, vol. 36, 2024.
- [4] J. Chen, D. Zhu, X. Shen, X. Li, Z. Liu, P. Zhang, R. Krishnamoorthi, V. Chandra, Y. Xiong, and M. Elhoseiny, “Minigt-v2: large language model as a unified interface for vision-language multi-task learning,” *arXiv preprint arXiv:2310.09478*, 2023.
- [5] J. Achiam, S. Adler, S. Agarwal, L. Ahmad, I. Akkaya, F. L. Aleman, D. Almeida, J. Altenschmidt, S. Altman, S. Anadkat *et al.*, “Gpt-4 technical report,” *arXiv preprint arXiv:2303.08774*, 2023.
- [6] C. Fu, R. Zhang, H. Lin, Z. Wang, T. Gao, Y. Luo, Y. Huang, Z. Zhang, L. Qiu, G. Ye *et al.*, “A challenger to gpt-4v? early explorations of gemini in visual expertise,” *arXiv preprint arXiv:2312.12436*, 2023.
- [7] H. Qin, G.-P. Ji, S. Khan, D.-P. Fan, F. S. Khan, and L. V. Gool, “How good is google bard’s visual understanding? an empirical study on open challenges,” *Machine Intelligence Research*, vol. 20, pp. 605–613, 2023.
- [8] Z. Gu, B. Zhu, G. Zhu, Y. Chen, M. Tang, and J. Wang, “Anomalygpt: Detecting industrial anomalies using large vision-language models,” *arXiv preprint arXiv:2308.15366*, 2023.
- [9] J. Qiu, L. Li, J. Sun, J. Peng, P. Shi, R. Zhang, Y. Dong, K. Lam, F. P.-W. Lo, B. Xiao, W. Yuan, N. Wang, D. Xu, and B. Lo, “Large ai models in health informatics: Applications, challenges, and the future,” *IEEE Journal of Biomedical and Health Informatics*, vol. 27, no. 12, pp. 6074–6087, 2023.
- [10] J. Zhang, X. Chen, Z. Xue, Y. Wang, C. Wang, and Y. Liu, “Exploring grounding potential of vqa-oriented gpt-4v for zero-shot anomaly detection,” *arXiv preprint arXiv:2311.02612*, 2023.
- [11] L. Tang, P.-T. Jiang, Z. Shen, H. Zhang, J. Chen, and B. Li, “Generalization and hallucination of large vision-language models through a camouflaged lens,” *arXiv preprint arXiv:2311.11273*, 2023.
- [12] H. Liu, C. Li, Y. Li, and Y. J. Lee, “Improved baselines with visual instruction tuning,” *arXiv preprint arXiv:2310.03744*, 2023.
- [13] K. Chen, Z. Zhang, W. Zeng, R. Zhang, F. Zhu, and R. Zhao, “Shikra: Unleashing multimodal llm’s referential dialogue magic,” *arXiv preprint arXiv:2306.15195*, 2023.
- [14] T.-Y. Lin, M. Maire, S. Belongie, J. Hays, P. Perona, D. Ramanan, P. Dollár, and C. L. Zitnick, “Microsoft coco: Common objects in context,” in *European Conference on Computer Vision*, 2014, pp. 740–755.
- [15] D.-P. Fan, M.-M. Cheng, J.-J. Liu, S.-H. Gao, Q. Hou, and A. Borji, “Salient objects in clutter: Bringing salient object detection to the foreground,” in *European Conference on Computer Vision*, 2018, pp. 186–202.
- [16] E. Xie, W. Wang, W. Wang, M. Ding, C. Shen, and P. Luo, “Segmenting transparent objects in the wild,” in *European Conference on Computer Vision*, 2020, pp. 696–711.
- [17] D.-P. Fan, G.-P. Ji, M.-M. Cheng, and L. Shao, “Concealed object detection,” *IEEE Transactions on Pattern Analysis and Machine Intelligence*, vol. 44, no. 10, pp. 6024–6042, 2021.
- [18] G.-P. Ji, D.-P. Fan, P. Xu, M.-M. Cheng, B. Zhou, and L. Van Gool, “Sam struggles in concealed scenes—empirical study on” segment anything,” *SCIENCE CHINA Information Sciences*, vol. 66, no. 12, pp. 226 101–, 2023.
- [19] N. C. Codella, D. Gutman, M. E. Celebi, B. Helba, M. A. Marchetti, S. W. Dusza, A. Kalloo, K. Liopyris, N. Mishra, H. Kittler *et al.*, “Skin lesion analysis toward melanoma detection: A challenge at the 2017 international symposium on biomedical imaging (isbi), hosted by the international skin imaging collaboration (isic),” in *IEEE International Symposium on Biomedical Imaging*, 2018, pp. 168–172.
- [20] N. Tajbakhsh, S. R. Gurudu, and J. Liang, “Automated polyp detection in colonoscopy videos using shape and context information,” *IEEE Transactions on Medical Imaging*, vol. 35, no. 2, pp. 630–644, 2015.
- [21] P. Bergmann, K. Batzner, M. Fauser, D. Sattlegger, and C. Steger, “The mvtec anomaly detection dataset: a comprehensive real-world dataset for unsupervised anomaly detection,” *International Journal of Computer Vision*, vol. 129, no. 4, pp. 1038–1059, 2021.
- [22] A. Conti, E. Fini, M. Mancini, P. Rota, Y. Wang, and E. Ricci, “Vocabulary-free image classification,” in *Advances in Neural Information Processing Systems*, vol. 36, 2024.
- [23] L. Wang, H. Lu, Y. Wang, M. Feng, D. Wang, B. Yin, and X. Ruan, “Learning to detect salient objects with image-level supervision,” in *IEEE Conference on Computer Vision and Pattern Recognition*, 2017, pp. 136–145.
- [24] J. Silva, A. Histace, O. Romain, X. Dray, and B. Granado, “Toward embedded detection of polyps in wce images for early diagnosis of colorectal cancer,” *International Journal of Computer Assisted Radiology and Surgery*, vol. 9, pp. 283–293, 2014.
- [25] W. Wang, J. Tian, C. Zhang, Y. Luo, X. Wang, and J. Li, “An improved deep learning approach and its applications on colonic polyp images detection,” *BMC Medical Imaging*, vol. 20, pp. 1–14, 2020.
- [26] Y. Zou, J. Jeong, L. Pemula, D. Zhang, and O. Dabeer, “Spot-the-difference self-supervised pre-training for anomaly detection and segmentation,” in *European Conference on Computer Vision*, 2022, pp. 392–408.
- [27] Y. Li, Y. Du, K. Zhou, J. Wang, W. X. Zhao, and J.-R. Wen, “Evaluating object hallucination in large vision-language models,” *arXiv preprint arXiv:2305.10355*, 2023.
- [28] P. Xu, W. Shao, K. Zhang, P. Gao, S. Liu, M. Lei, F. Meng, S. Huang, Y. Qiao, and P. Luo, “Lvlm-ehub: A comprehensive evaluation benchmark for large vision-language models,” *arXiv preprint arXiv:2306.09265*, 2023.
- [29] C. Cui, Y. Zhou, X. Yang, S. Wu, L. Zhang, J. Zou, and H. Yao, “Holistic analysis of hallucination in gpt-4v (ision): Bias and interference challenges,” *arXiv preprint arXiv:2311.03287*, 2023.
- [30] A. Kirillov, E. Mintun, N. Ravi, H. Mao, C. Rolland, L. Gustafson, T. Xiao, S. Whitehead, A. C. Berg, W.-Y. Lo, P. Dollar, and R. Girshick, “Segment anything,” in *IEEE International Conference on Computer Vision*, 2023, pp. 4015–4026.
- [31] A. Dosovitskiy, L. Beyer, A. Kolesnikov, D. Weissenborn, X. Zhai, T. Unterthiner, M. Dehghani, M. Minderer, G. Heigold, S. Gelly *et al.*, “An image is worth 16x16 words: Transformers for image recognition at scale,” *arXiv preprint arXiv:2010.11929*, 2020.
- [32] R. Padilla, W. L. Passos, T. L. B. Dias, S. L. Netto, and E. A. B. da Silva, “A comparative analysis of object detection metrics with a companion open-source toolkit,” *Electronics*, vol. 10, 2021.
- [33] F. Perazzi, P. Krähenbühl, Y. Pritch, and A. Sorkine-Hornung, “Saliency filters: Contrast based filtering for salient region detection,” in *IEEE Conference on Computer Vision and Pattern Recognition*, 2012, pp. 733–740.
- [34] D.-P. Fan, M.-M. Cheng, Y. Liu, T. Li, and A. Borji, “Structure-measure: A new way to evaluate foreground maps,” in *IEEE International Conference on Computer Vision*, 2017, pp. 4558–4567.
- [35] R. Achanta, S. Hemami, F. Estrada, and S. Susstrunk, “Frequency-tuned salient region detection,” in *IEEE Conference on Computer Vision and Pattern Recognition*, 2009, pp. 1597–1604.
- [36] J. Gu, Z. Han, S. Chen, A. Beirami, B. He, G. Zhang, R. Liao, Y. Qin, V. Tresp, and P. Torr, “A systematic survey of prompt engineering on vision-language foundation models,” *arXiv preprint arXiv:2307.12980*, 2023.
- [37] C. Li, C. Wong, S. Zhang, N. Usuyama, H. Liu, J. Yang, T. Naumann, H. Poon, and J. Gao, “Llava-med: Training a large language-and-vision assistant for biomedicine in one day,” in *Advances in Neural Information Processing Systems*, vol. 36, 2024.
- [38] Y. Zhou, C. Cui, J. Yoon, L. Zhang, Z. Deng, C. Finn, M. Bansal, and H. Yao, “Analyzing and mitigating object hallucination in large vision-language models,” *arXiv preprint arXiv:2310.00754*, 2023.
- [39] Y. Qian, H. Zhang, Y. Yang, and Z. Gan, “How easy is it to fool your multimodal llms? an empirical analysis on deceptive prompts,” *arXiv preprint arXiv:2402.13220*, 2024.
- [40] J. M. Kim, A. Koepke, C. Schmid, and Z. Akata, “Exposing and mitigating spurious correlations for cross-modal retrieval,” in *IEEE Conference on Computer Vision and Pattern Recognition*, 2023, pp. 2584–2594.
- [41] Y. Wu, Y. Zhao, Z. Li, B. Qin, and K. Xiong, “Improving cross-task generalization with step-by-step instructions,” *SCIENCE CHINA Information Sciences*, 2023.
- [42] H. Chen, K. Yuan, Y. Huang, L. Guo, Y. Wang, and J. Chen, “Feedback is all you need: from chatgpt to autonomous driving,” *SCIENCE CHINA Information Sciences*, vol. 66, no. 6, pp. 1–3, 2023.
- [43] S. Yan, M. Bai, W. Chen, X. Zhou, Q. Huang, and L. E. Li, “Vigor: Improving visual grounding of large vision language models with fine-grained reward modeling,” *arXiv preprint arXiv:2402.06118*, 2024.

- [44] Q. Jiao, D. Chen, Y. Huang, Y. Li, and Y. Shen, "Enhancing multimodal large language models with vision detection models: An empirical study," *arXiv preprint arXiv:2401.17981*, 2024.